WMO
GREENHOUSE GAS BULLETIN

The State of Greenhouse Gases in the Atmosphere
Based on Global Observations through 2013
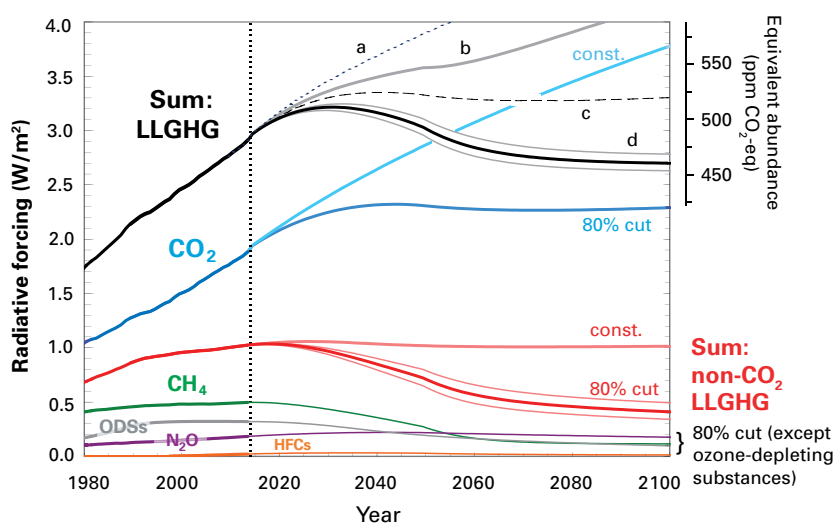
World Meteorological Organization
Weather · Climate · Water

GLOBAL ATMOSPHERE WATCH

No. 10 | 9 September 2014

Climate Summit Edition

The WMO Global Atmosphere Watch (GAW) coordinates observations of the most important contributors to climate change: long-lived greenhouse gases (LLGHG). In the figure, their radiative forcing (RF) is plotted along with a simple illustration of the impacts on future RF of different emission reduction scenarios. Analysis of GAW observations shows that a reduction in RF from its current level ($2.92 \ W \cdot m^{-2}$ in 2013)[1] requires significant reductions in anthropogenic emissions of all major greenhouse gases (GHGs).

Long-lived GHGs (carbon dioxide (CO_2), methane (CH_4), nitrous oxide (N_2O), substances that deplete stratospheric ozone), and remaining gases listed under the Kyoto Protocol to the United Nations Framework Convention on Climate Change (sulphur hexafluoride (SF_6), hydrofluorocarbons (HFCs) and perfluorocarbons (PFCs)) are the main drivers of climate change, and WMO GAW monitors them all. WMO GAW atmospheric measurements of these gases are used to inform climate policy in two ways: (1) The observations are compared with determinations of LLGHG atmospheric abundances from pre-industrial times (usually 1750) from ice cores to calculate RF (defined as the change in Earth's net radiative flux); (2) For gases that do not exchange rapidly between the atmosphere and ocean or biosphere, the observations are combined with estimates of LLGHG lifetimes to quantify their emissions. The figure above uses both pieces of information. It shows the increase in RF above its pre-industrial level for the major LLGHGs from 1980 through 2013 (see plots of data and their descriptions in this bulletin) and their sum (in black), and it illustrates the change in RF that would occur from 2014–2100 based on emission reductions as follows: (a) emissions held constant at 2013 levels, (b) constant CO_2 emissions and 80% reduction in anthropogenic non-CO_2 GHG emissions, (c) 80% reduction in CO_2 emissions while non-CO_2 GHG emissions are held constant, and (d) 80% reductions in all LLGHG emissions. The projections are not based on realistic emissions scenarios; they merely illustrate that achieving reductions in RF will require significant decreases in anthropogenic emissions of both non-CO_2 LLGHGs and CO_2. The figure and description are based on an update of Montzka et al. (2011).

Executive summary

The latest analysis of observations from the WMO Global Atmosphere Watch Programme shows that the globally averaged mole fractions of CO_2, CH_4 and N_2O reached new highs in 2013, with CO_2 at 396.0±0.1 ppm[2], CH_4 at 1824±2 ppb[3] and N_2O at 325.9±0.1 ppb. These values constitute, respectively, 142%, 253% and 121% of pre-industrial (before 1750) levels. The atmospheric increase of CO_2 from 2012 to 2013 was 2.9 ppm, which is the largest year to year change from 1984 to 2013. For N_2O the increase from 2012 to 2013 is smaller than the one observed from 2011 to
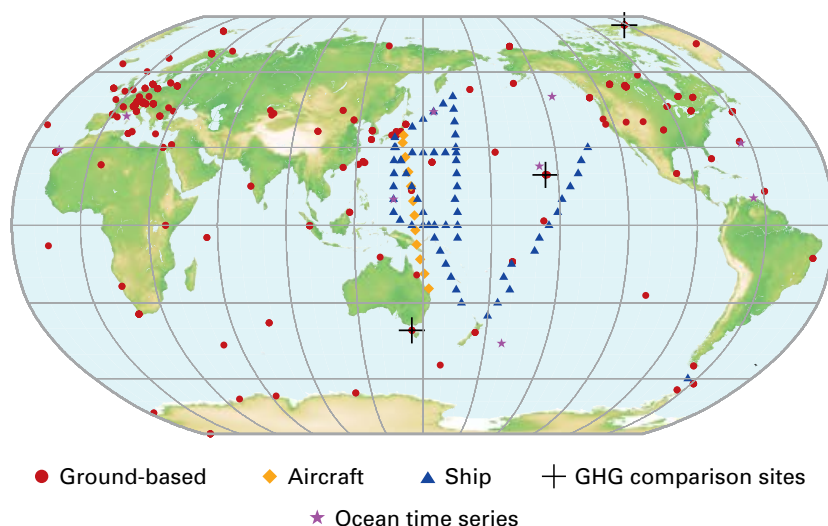
Figure 2. The GAW global network for carbon dioxide in the last decade. The network for methane is similar. Also shown are featured locations where observations of CO_2 are performed in ocean water.
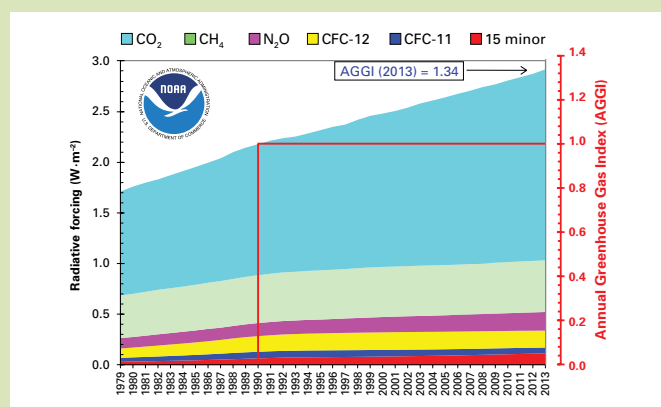

Figure 1. Atmospheric radiative forcing, relative to 1750, of LLGHGs and the 2013 update of the NOAA Annual Greenhouse Gas Index (AGGI)

Table 1. Global annual mean abundances (2013) and trends of key greenhouse gases from the WMO/GAW global greenhouse gas monitoring network. Units are dry-air mole fractions, and uncertainties are 68% confidence limits.

	CO_2	CH_4	N_2O
Global abundance in 2013[4]	396.0±0.1 ppm	1824±2 ppb	325.9±0.1 ppb
2013 abundance relative to year 1750[a]	142%	253%	121%
2012–2013 absolute increase	2.9 ppm	6 ppb	0.8 ppb
2012–2013 relative increase	0.74%	0.33%	0.25%
Mean annual absolute increase during last 10 years	2.07 ppm/yr	3.8 ppb/yr	0.82 ppb/yr

[a] Assuming a pre-industrial mole fraction of 278 ppm for CO_2, 722 ppb for CH_4 and 270 ppb for N_2O. Stations used for the analyses numbered 124 for CO_2, 121 for CH_4 and 33 for N_2O. (An updated pre-industrial CH_4 value was used compared with previous bulletins, which slightly reduces radiative forcing and the relative increase in CH_4 relative to 1750. It had no impact on the AGGI.)

2012 but comparable to the average growth rate over the past 10 years. Atmospheric CH_4 continued to increase at a rate similar to the mean rate over the past five years. The National Oceanic and Atmospheric Administration (NOAA) Annual Greenhouse Gas Index shows that from 1990 to 2013 radiative forcing by long-lived greenhouse gases increased by 34%, with CO_2 accounting for about 80% of this increase. Uptake of anthropogenic CO_2 by the ocean led to increased CO_2 concentrations and increased acidity levels in seawater. During the last two decades ocean water acidity expressed as pH decreased by 0.0011–0.0024 units per year, and the amount of CO_2 dissolved in seawater (pCO_2) increased by 1.2–2.8 µatm per year for time series from several featured ocean stations.

Overview

This tenth WMO/GAW Annual GHG Bulletin reports atmospheric abundances and rates of change of the most important long-lived greenhouse gases – carbon dioxide, methane and nitrous oxide – and provides a summary of the contributions of the other gases. These three, together with CFC-12 and CFC-11, account for approximately 96%[5] of radiative forcing due to LLGHGs (Figure 1). For the first time, this bulletin contains a section on ocean acidification prepared in collaboration with the International Ocean Carbon Coordination Project (IOCCP) of the Intergovernmental Oceanographic Commission of the United Nations Educational, Scientific and Cultural Organization (IOC-UNESCO), the Scientific Committee on Oceanic Research (SCOR), and the Ocean Acidification International Coordination Centre (OA-ICC) of the International Atomic Energy Agency (IAEA).

The WMO Global Atmosphere Watch Programme (http://www.wmo.int/gaw) coordinates systematic observations and analysis of atmospheric greenhouse gases and other trace species. Sites where greenhouse gases are monitored in the last decade are shown in Figure 2. This map includes several featured stations where observations of CO_2 in ocean water are performed. Atmospheric measurement data are reported by participating institutions and archived and distributed by the World Data Centre for Greenhouse Gases (WDCGG) at the Japan Meteorological Agency.
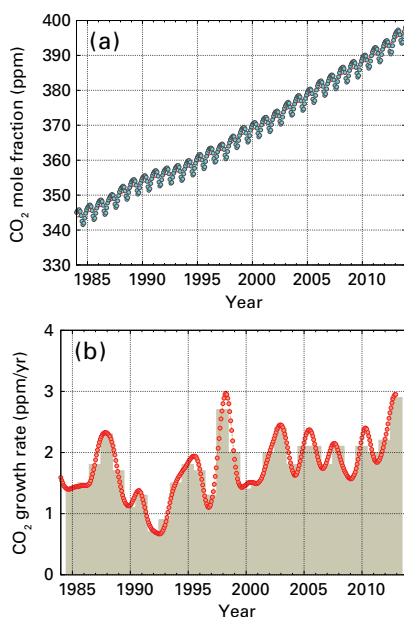
Figure 3. Globally averaged CO_2 mole fraction (a) and its growth rate (b) from 1984 to 2013. Differences in successive annual means are shown as shaded columns in (b).

Figure 4. Globally averaged CH_4 mole fraction (a) and its growth rate (b) from 1984 to 2013. Differences in successive annual means are shown as shaded columns in (b).

Figure 5. Globally averaged N_2O mole fraction (a) and its growth rate (b) from 1984 to 2013. Differences in successive annual means are shown as shaded columns in (b).
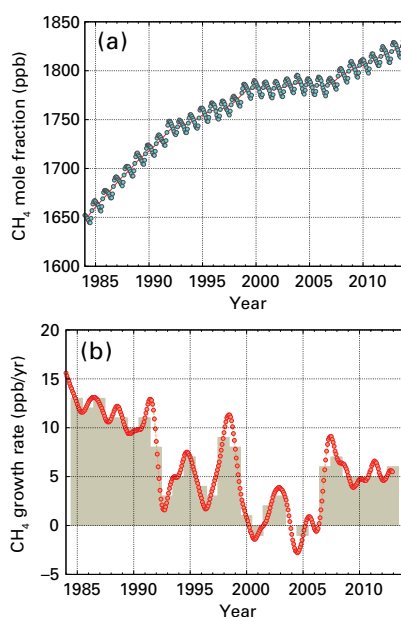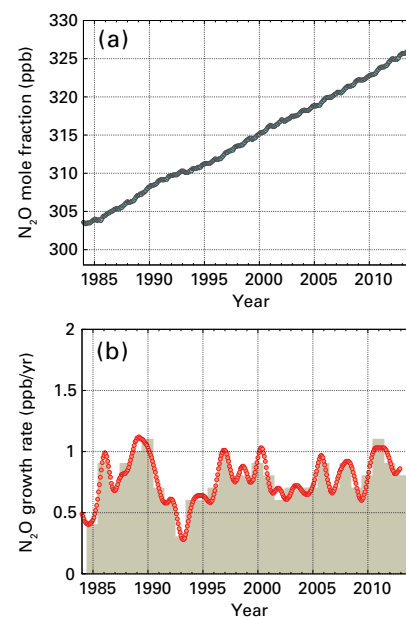
Table 1 provides globally averaged atmospheric abundances of the three major LLGHGs in 2013 and changes in their abundances since 2012 and 1750. The results are obtained from an analysis of datasets (WMO, 2009) that are traceable to WMO World Reference Standards. Data from mobile stations, with the exception of NOAA sampling onboard ships transecting the Pacific Ocean, are not used for this global analysis.

The three greenhouse gases shown in Table 1 are closely linked to anthropogenic activities and they also interact strongly with the biosphere and the oceans. Predicting the evolution of the atmospheric content of greenhouse gases requires quantitative understanding of their many sources, sinks and chemical transformations in the atmosphere. Observations from GAW provide invaluable constraints on the budgets of these and other LLGHGs, and they are used to verify emission inventories and evaluate satellite retrievals of LLGHG column averages.

The NOAA Annual Greenhouse Gas Index in 2013 was 1.34, representing a 34% increase in total radiative forcing (relative to 1750) by all LLGHGs since 1990 and a 1.5% increase from 2012 to 2013 (Figure 1). The total radiative forcing by all LLGHGs in 2013 corresponds to a CO_2-equivalent mole fraction of 479 ppm. (http://www.esrl.noaa.gov/gmd/aggi).

Carbon dioxide (CO_2)

Carbon dioxide is the single most important anthropogenic greenhouse gas in the atmosphere, contributing ~65%[5] to radiative forcing by LLGHGs. It is responsible for ~84% of the increase in radiative forcing over the past decade and ~83% over the past five years. The pre-industrial level of ~278 ppm represented a balance of relatively large annual two-way fluxes between the atmosphere and oceans (~80 PgC yr^{-1}) and the atmosphere and terrestrial biosphere (~120 PgC yr^{-1}). Atmospheric CO_2 reached 142% of the pre-industrial level in 2013, primarily because of emissions from combustion of fossil fuels and cement production (CO_2 emissions were 9.7±0.5 PgC[6] in 2012, according to http://www.globalcarbonproject.org). This conclusion is consistent with GAW measurements of the spatial distribution of CO_2 at the Earth's surface and its rate of increase, a decrease in the abundance of atmospheric oxygen (O_2), and a decrease in carbon isotope ratio, $^{13}C/^{12}C$, in atmospheric CO_2. Minor contributions to increased CO_2 come from deforestation and other land-use change (1.0±0.5 PgC in 2012), although the net effect of terrestrial biosphere fluxes is as a sink. The average increase in atmospheric CO_2 from 2003 to 2013 corresponds to ~45% of the CO_2 emitted by human activity with the remaining ~55% removed by the oceans and the terrestrial biosphere. The main sinks for CO_2 emissions from fossil fuel combustion are the oceans and terrestrial biosphere. Knowledge of partitioning between these sinks is based on GAW observations of atmospheric CO_2 and O_2. Uptake of atmospheric CO_2 by the oceans results in ocean acidification (see next page).

Globally averaged CO_2 in 2013 was 396.0±0.1 ppm (Figure 3 (a)). The increase in global annual mean CO_2 from 2012 to 2013 of 2.9 ppm is greater than the increase from 2011 to 2012, the average growth rate for the 1990s (~1.5 ppm yr^{-1}), and the average growth rate for the past decade (~2.1 ppm yr^{-1}). Recent increases in emissions of CO_2 from fossil fuel combustion (~2% yr^{-1} or ~0.2 PgC yr^{-1}) cannot explain the interannual variability in CO_2 growth rate nor the greater-than-average increase in annual means from 2012 to 2013. Measurements of $^{13}C/^{12}C$ in atmospheric CO_2 by GAW participants indicate that changes in CO_2 growth rate result

OCEAN ACIDIFICATION

The ocean currently absorbs one fourth of anthropogenic CO_2 emissions, reducing the increase in atmospheric CO_2 that would otherwise occur because of fossil fuel combustion. Enhanced ocean CO_2 uptake alters the marine carbonate system that controls seawater acidity. As CO_2 dissolves in seawater it forms carbonic acid (H_2CO_3), a weak acid that dissociates into bicarbonate (HCO_3^-) and hydrogen ions (H^+). Increased H^+ means increased acidity (lower pH). The ocean's acidity increase is already measurable as oceans take up ~4 kg CO_2 per day per person. The rate of acidification is limited by the presence of carbonate ion (CO_3^{2-}), which binds up most of the newly formed H^+, forming bicarbonate. Yet that buffering reaction consumes CO_3^{2-}, reducing the chemical capacity of the near-surface ocean to take up more CO_2. Currently that capacity is only 70% of what it was at the beginning of the industrial era, and it may well be reduced to only 20% by the end of the twenty-first century. The current rate of ocean acidification appears unprecedented at least over the last 300 million years, based on proxy-data from paleo archives. Acidification will continue to accelerate at least until mid-century, based on projections from Earth system models. Acidification rates are slightly affected by climate change, but those effects amount to less than 10% of the changes due to increasing CO_2. Yet freshening, for example from enhanced ice melt in the Arctic, can significantly accelerate acidification rates.

Whereas the chemistry of ocean acidification is generally well understood from observations and models, the potential consequences of ocean acidification on marine organisms are inherently more complicated. A major concern is the response of calcifying organisms, such as corals, coralline algae, mollusks and some plankton, because their ability to build shell or skeletal material (via calcification) depends on the abundance of CO_3^{2-}. For many organisms, calcification declines with increased acidification. Other impacts of acidification on marine biota include reduced survival, development and growth rates, as well as changes in physiological functions and reduced biodiversity.

The decrease in surface ocean pH and increase in the surface partial pressure of CO_2 (pCO_2) due to ocean uptake of anthropogenic carbon is already detectable. These trends have been assessed and quantified by sustained ocean-time-series observations, which provide the long, temporally resolved datasets needed to characterize changes in ocean biogeochemistry and ecosystems. Examples of such time series are presented in Figure 6 and Table 2. At all locations (>10 years of measurements), surface pCO_2 has increased with time due to the rise of anthropogenic CO_2, accompanied by a corresponding acidification. These time-series stations generally represent large regions, from subpolar (MUNIDA, Station P and KNOT/K2) to subtropical (BATS, HOT, ESTOC, DYFAMED) and tropical (CARIACO, 137°E section). De-seasonalized surface data from these time series were used and a linear trend was fit over the range of measurements to provide comparable decadal changes for these stations. While there are seasonal and interannual variations, pCO_2 has increased at a rate of 1.2–2.8 µatm yr^{-1} (the atmospheric mole fraction increased at an average rate of 2.1 ppm yr^{-1} during the last 10 years), while ocean surface pH has decreased during the period of observations at an average rate of -0.0011 yr^{-1} to -0.0024 yr^{-1}, depending on the location. The rate of these changes depends not only on the chemistry but also on other factors particular to each region. At ESTOC, HOT and BATS, the rates of increase in surface pCO_2 match the rise in atmospheric pCO_2. Similarly, the pH decrease has been steady, consistent with the rate of acidification expected from equilibration with the atmosphere. At 10°N in the 137°E section, the rise of pCO_2 and decrease of pH was slightly lower, potentially linked to changes in the circulation of the subtropical gyre. The DYFAMED time series has experienced circulation changes overlapping a strong seasonal signal, which leads to large error-bars on the linear trend. At CARIACO, surface pCO_2 was one of the highest measured, particularly during times of upwelling of CO_2-rich waters. Its large increase in pCO_2 and decrease in pH over time can be attributed to warming of surface waters linked to a reduction in upwelling, which leads to lower biological productivity. The subpolar time series displayed some of the highest extremes, caused in part by the large seasonal differences in temperature and biological productivity. At MUNIDA, the rate of increase of surface pCO_2 was low, whereas at KNOT/K2, pCO_2 increase was similar to the atmospheric rise; however, pH decrease at KNOT/K2 was one of the greatest. Sampling at Station P has not been as regular, but decreases in pH and increases in pCO_2 follow similar trends as at the other sites.

While the focus here is on surface observations, a large portion of the water column is being affected by anthropogenic carbon uptake and associated changes in ocean chemistry. Unfortunately, there are currently only a few time-series stations that conduct CO_2 measurements and this poses significant obstacles to quantifying trends in ocean acidification and carbonate chemistry. CO_2 observations from time-series stations, together with surface and interior ocean measurements from ships, need to be sustained and extended.
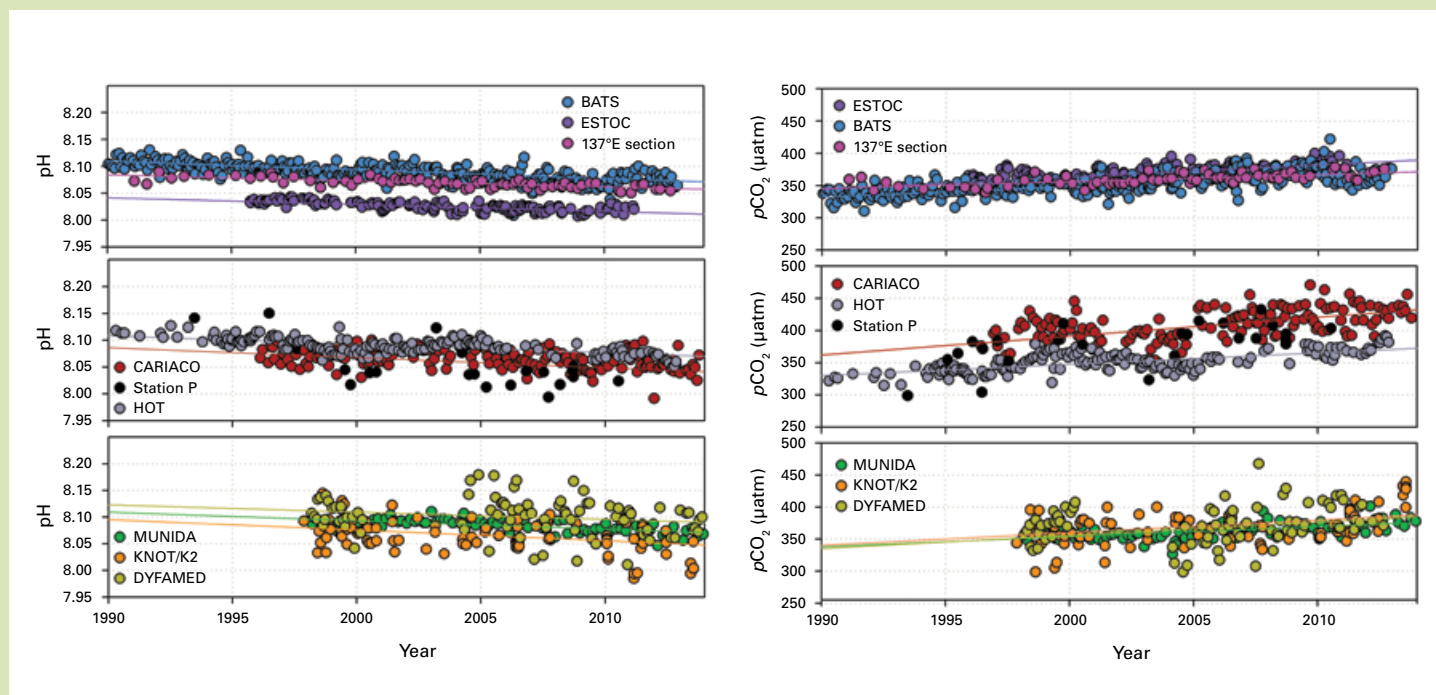
Figure 6. Time series of de-seasonalized surface seawater pH and respective trendlines (left) and of de-seasonalized surface pCO_2 (µatm) and respective trendlines (right). Featured time series include the Bermuda Atlantic Time-series Study (BATS; blue) the European Station for Time Series in the Ocean near the Canary Islands (ESTOC; purple), the Hawaii Ocean Time-series (HOT; grey); CARIACO (red); Station P (black); MUNIDA (green); the Kyodo North Pacific Time series (KNOT; orange); the station known as the Dynamics of Atmospheric Fluxes in the MEDiterranean Sea (DYFAMED; yellow); the Japan Meteorological Agency 137°E section repeat hydrographic line at 10°N, 137°E (137°E section; pink). The locations of the featured time series are shown in Figure 2. Temporal sampling resolution varies from monthly to annually.

Table 2. Linear trends and standard errors for surface pH[a] and pCO_2 at the nine featured ocean time series

Time series	pH (yr^{-1})	pCO_2 (µatm yr^{-1})	Reference
BATS[b]	−0.0017±0.0001	1.75±0.08	Bates et al., 2014
ESTOC[b]	−0.0014±0.0001	1.78±0.15	Bates et al., 2014 González-Dávila et al., 2010
HOT[b]	−0.0017±0.0001	1.89±0.15	Bates et al., 2014 Dore et al., 2009
CARIACO[b]	−0.0024±0.0003	2.79±0.37	Bates et al., 2014 Astor et al., 2013
DYFAMED[b]	−0.0019±0.0009	2.56±0.85	Touratier and Goyet, 2011
MUNIDA[b]	−0.0016±0.0003	1.55±0.24	Bates et al., 2014 Currie et al., 2011
KNOT/K2[b]	−0.0024±0.0007	2.22±0.67	Wakita et al., 2013
Station P[c]	c	c	Wong et al., 2010
137°E section at 10°N[d]	−0.0011±0.0001	1.15±0.06	Midorikawa et al., 2010

[a] pH in total hydrogen ion concentration scale at in situ temperatures.

[b] Data of pH and pCO_2 were calculated from measurements of total dissolved inorganic carbon, total alkalinity, temperature and salinity (silicate and phosphate assumed to be zero), except for those instances where direct measurements of pH were available. De-seasonalized data and linear trends were calculated according to GAW Report No. 184.

[c] Too few data are available for Station P for a linear trend calculation.

[d] Data of pH were calculated from measurements of pCO_2 and total dissolved inorganic carbon, temperature and salinity.

from small changes in fluxes between the atmosphere and terrestrial biosphere. Typically, ~120 PgC is exchanged between the atmosphere and terrestrial biosphere each year. This accounts for the observed seasonal cycle in atmospheric CO_2 abundance in the northern hemisphere. Small interannual variability (1–2%) in these fluxes, either from a change in the balance between photosynthesis and respiration or the amount of biomass burned, have a large impact on the growth rate of CO_2 (~4 PgC yr^{-1}). It is too early to say which factors are responsible for the larger-than-average increase in annual means from 2012 to 2013, but this active area of research relies on measurements by GAW participants.

Methane (CH₄)

Methane contributes ~17%[5] to radiative forcing by LLGHGs. Approximately 40% of methane is emitted into the atmosphere by natural sources (e.g. wetlands and termites), and about 60% comes from anthropogenic sources (e.g. ruminants, rice agriculture, fossil fuel exploitation, landfills and biomass burning). As a result of increased anthropogenic emissions, atmospheric CH_4 reached 253% of its pre-industrial level (~722 ppb) in 2013. Atmospheric CH_4 increased from ~1650 ppb in the early 1980s to a new high of 1824±2 ppb in 2013 (Figure 4 (a)). Its growth rate (Figure 4 (b)) decreased from ~13 ppb yr^{-1} during the early 1980s to near zero during 1999–2006. Superimposed on top of the long-term changes in growth rate is significant interannual variability (IAV). Studies of IAV help understand the processes that contribute to CH_4 emissions and losses. Since 2007, atmospheric CH_4 has been increasing again; its global annual mean increased by 6 ppb from 2012 to 2013. Studies using GAW CH_4 measurements indicate that increased CH_4 emissions from wetlands in the tropics and from anthropogenic sources at mid-latitudes of the northern hemisphere are likely causes. As shown in WMO Greenhouse Gas Bulletin No. 9, increased emissions from the Arctic did not contribute to the continued increase in atmospheric CH_4 since 2007.

Nitrous oxide (N₂O)

Nitrous oxide contributes ~6%[5] to radiative forcing by LLGHGs. It is the third most important contributor to LLGHG radiative forcing and has the largest emissions of substances that deplete stratospheric ozone (O_3) when weighted by ozone-depleting potential. Prior to industrialization, the atmospheric N_2O burden reflected a balance between emissions from soils and the ocean, and chemical losses in the stratosphere. In the industrial era, additional anthropogenic emissions are from synthetic nitrogen fertilizers (direct emissions from agricultural fields and indirect emissions from waterways affected by agricultural runoff), fossil fuel combustion, biomass burning and other minor processes. Currently, anthropogenic sources emit ~40% of total emissions; that total, determined from GAW measurements of globally averaged N_2O (Figure 5 (a)) and its rate of increase in recent years (Figure 5 (b)), is about 16 TgN yr^{-1}.[7] Synthetic nitrogen fertilizers are the largest contributor to the increase since pre-industrial times. The globally averaged N_2O mole fraction in 2013 reached 325.9±0.1 ppb, which is 0.8 ppb greater than the previous year and 121% of the pre-industrial level (270 ppb). The increase in annual means

from 2012 to 2013 is comparable to the mean growth rate over the past 10 years (0.82 ppb yr^{-1}).

GAW N_2O measurements have been used with atmospheric chemical transport models to estimate emissions at regional to continental spatial scales. Recent studies have identified tropical and subtropical land regions as the largest source regions (Thompson et al., 2014) and significant trends in N_2O emissions from Asia (Saikawa et al., 2014). Despite these advances in understanding the N_2O budget, improvements to inter-network compatibility of measurements by GAW participants are necessary. Because atmospheric N_2O has a long atmospheric lifetime (130 yr), spatial gradients are small. So, to infer estimates of emissions from the data using a transport model, biases among measurement programmes must be small, <0.1 ppb, a target that is difficult to reach with commonly used measurement technologies.
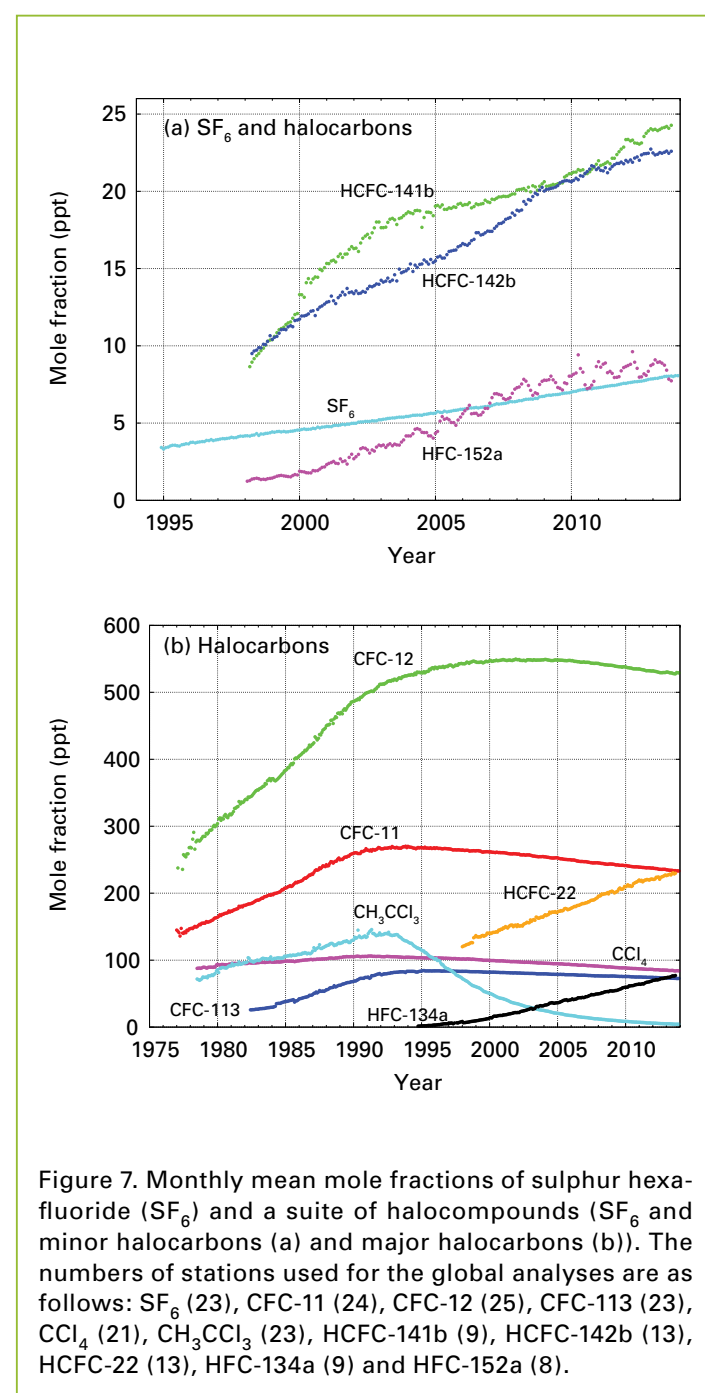

Figure 7. Monthly mean mole fractions of sulphur hexafluoride (SF_6) and a suite of halocompounds (SF_6 and minor halocarbons (a) and major halocarbons (b)). The numbers of stations used for the global analyses are as follows: SF_6 (23), CFC-11 (24), CFC-12 (25), CFC-113 (23), CCl_4 (21), CH_3CCl_3 (23), HCFC-141b (9), HCFC-142b (13), HCFC-22 (13), HFC-134a (9) and HFC-152a (8).

6

Other greenhouse gases

Sulphur hexafluoride is a potent LLGHG. Its emissions are almost entirely anthropogenic, and it is used mainly as an electrical insulator in power distribution equipment. Its current mole fraction is about twice the level observed in the mid-1990s (Figure 7 (a)). It has a very long atmospheric lifetime, 3 200 yr, so emissions accumulate in the atmosphere and can be determined from the rate of increase measured by GAW participants. An analysis of observations shows that emissions reported to the United Nations Framework Convention on Climate Change are greatly underestimated and are not consistent with atmospheric measurements (Levin et al., 2010). GAW SF_6 observations have another important use: they validate atmospheric mixing used in chemical transport models as described above for N_2O.

The stratospheric ozone-depleting chlorofluorocarbons (CFCs), together with minor halogenated gases, contribute ~12%[5] to radiative forcing by LLGHGs. While CFCs and most halons are decreasing, hydrochlorofluorocarbons (HCFCs) and hydrofluorocarbons (HFCs), which are also potent greenhouse gases, are increasing at relatively rapid rates, although they are still low in abundance (at ppt[8] levels, Figure 7 (a) and (b)).

This bulletin primarily addresses LLGHGs. Relatively short-lived tropospheric ozone has a radiative forcing comparable to that of the halocarbons. Many other pollutants, such as carbon monoxide, nitrogen oxides and volatile organic compounds, although not referred to as greenhouse gases, have small direct or indirect effects on radiative forcing. Aerosols (suspended particulate matter), too, are short-lived substances that alter the radiation budget. All gases mentioned herein, as well as aerosols, are monitored by the GAW Programme, with support from WMO Member countries and contributing networks.

Distribution of the bulletins

The WMO Secretariat prepares and distributes these bulletins in cooperation with the World Data Centre for Greenhouse Gases at the Japan Meteorological Agency and the GAW Scientific Advisory Group for Greenhouse Gases, with the assistance of the NOAA Earth System Research Laboratory (ESRL). The bulletins are available through the GAW Programme or the WDCGG web page.

Acknowledgements and links

Fifty WMO member countries have contributed CO_2 data to the GAW WDCGG. Approximately 46% of the measurement records submitted to WDCGG are obtained at sites of the NOAA ESRL cooperative air-sampling network. For other networks and stations, see GAW Report No. 206 (available at http://www.wmo.int/gaw). The Advanced Global Atmospheric Gases Experiment (AGAGE) also contributed observations to this bulletin. Furthermore, the GAW monitoring stations contributing data to this bulletin, shown in Figure 2, are included in the list of contributors on the WDCGG web page (http://ds.data.jma. go.jp/gmd/wdcgg/).They are also described in the GAW Station Information System, GAWSIS (http://gaw.empa. ch/gawsis) supported by MeteoSwiss, Switzerland.

The summary on ocean acidification and trends in ocean pCO$_2$ was jointly produced by the International Ocean Carbon Coordination Project of the Intergovernmental Oceanographic Commission of UNESCO, the Scientific Committee on Oceanic Research, and the Ocean Acidification International Coordination Centre of the International Atomic Energy Agency with support from WMO. Particular thanks go to Y. Astor, N. Bates, M. Church, L. Coppola, K. Currie, M. González-Dávila, L. Miller, T. Nakano and M. Wakita for their time-series data contribution and interpretation.

References

Astor, Y.M., L. Lorenzoni, R. Thunell, R. Varela, F. Muller-Karger, L. Troccoli, G.T. Taylor, M.I. Scranton, E. Tappa and D. Rueda, 2013: Interannual variability in sea surface temperature and fCO$_2$ changes in the Cariaco Basin. *Deep-Sea Res. II*, 93:33–43, doi:10.1016/j.dsr.2013.01.002.

Bates, N.R., Y.M. Astor, M.J. Church, K. Currie, J.E. Dore, M. González-Dávila, L. Lorenzoni, F. Muller-Karger, J. Olafsson and J.M. Santana-Casiano, 2014: A time-series view of changing ocean chemistry due to ocean uptake of anthropogenic CO$_2$ and ocean acidification. *Oceanography.* 27(1):126–141, http://dx.doi.org/10.5670/oceanog.2014.16.

Conway, T.J., P.P. Tans, L.S. Waterman, K.W. Thoning, D.R. Kitzis, K.A. Masarie and Ni Zhang, 1994: Evidence for interannual variability of the carbon cycle from the National Oceanic and Atmospheric Administration/Climate Monitoring and Diagnostics Laboratory global air sampling network. *J. Geophys. Res.*, 99(D11):22831–22855.

Currie, K.I., M.R. Reid and K.A. Hunter, 2011: Interannual variability of carbon dioxide drawdown by subantarctic surface water near New Zealand. *Biogeochemistry*, 104(1–3):23–34, doi:10.1007/s10533-009-9355-3.

Dore, J.E., R. Lukas, D.W. Sadler, M.J. Church and D.M. Karl, 2009: Physical and biogeochemical modulation of ocean acidification in the central North Pacific. *PNAS*, 106(30):12235–12240, doi:10.1073/pnas.0906044106.

González-Dávila, M., J.M. Santana-Casiano, M.J. Rueda and O. Llinás, 2010: The water column distribution of carbonate system variables at the ESTOC site from 1995 to 2004. *Biogeosciences*, 7:3067–3081, doi:10.5194/bg-7-3067-2010.

Levin, I., T. Naegler, R. Heinz, D. Osusko, E. Cuevas, A. Engel, J. Ilmberger, R.L. Langenfelds, B. Neininger, C. v. Rohden, L.P. Steele, R. Weller, D.E. Worthy, and S.A. Zimov, 2010: The global SF$_6$ source inferred from long-term high precision atmospheric measurements and its comparison with emission inventories. *Atmos. Chem. Phys.*, 10(6):2655–2662, doi:10.5194/acp-10-2655-2010.

Midorikawa, T., M.A. Ishii, S. Saito, D. Sasano, N. Kosugi, T. Motoi, H. Kamiya, A. Nakadate, K. Nemoto and H.Y. Inoue, 2010: Decreasing pH trend estimated from 25-yr time series of carbonate parameters in the western North Pacific. *Tellus B*, 62:649–659. Updated based on: http://www.data.jma.go.jp/gmd/kaiyou/english/co2_trend/co2_trend_en.html; http://www.data.jma.go.jp/gmd/kaiyou/english/oa/oceanacidification_en.html.

Montzka, S.A., E.J. Dlugokencky and J.H. Butler, 2011: Non-CO$_2$ greenhouse gases and climate change. *Nature,* 476:43–50, doi:10.1038/nature10322.

Saikawa, E., R.G. Prinn, E. Dlugokencky, K. Ishijima, G.S. Dutton, B.D. Hall, R. Langenfelds, Y. Tohjima,

T. Machida, M. Manizza, M. Rigby, S. O'Doherty, P.K. Patra, C.M. Harth, R.F. Weiss, P.B. Krummel, M. van der Schoot, P.J. Fraser, L.P. Steele, S. Aoki, T. Nakazawa, and J.W. Elkins, 2014: Global and regional emissions estimates for N_2O. *Atmos. Chem. Phys.*, 14(9):4617–4641, doi:10.5194/acp-14-4617-2014.

Thompson, R.L., F. Chevallier, A.M. Crotwell, G. Dutton, R.L. Langenfelds, R.G. Prinn, R.F. Weiss, Y. Tohjima, T. Nakazawa, P.B. Krummel, L.P. Steele, P. Fraser, S. O'Doherty, K. Ishijima and S Aoki, 2014: Nitrous oxide emissions 1999 to 2009 from a global atmospheric inversion. *Atmos. Chem. Phys.*, 14(4):1801–1817, doi:10.5194/acp-14-1801-2014.

Touratier, F. and C. Goyet, 2011: Impact of the Eastern Mediterranean Transient on the distribution of anthropogenic CO_2 and first estimate of acidification of the Mediterranean Sea. *Deep-Sea Research I*, 58(1):1–15, doi: 10.1016/j.dsr.2010.10.002.

Wakita, M., S. Watanabe, M. Honda, A. Nagano, K. Kimoto, K. Matsumoto, M. Kitamura, K. Sasaki, H. Kawakami, T. Fujiki, K. Sasaoka, Y. Nakano and A. Murata, 2013: Ocean acidification from 1997 to 2011 in the subarctic western North Pacific Ocean. *Biogeosciences*, 10:7817–7827, doi:10.5194/bg-10-7817-2013.

WMO, 2009: *Technical Report of Global Analysis Method for Major Greenhouse Gases by the World Data Centre for Greenhouse Gases* (Y. Tsutsumi, K. Mori, T. Hirahara, M. Ikegami and T.J. Conway). GAW Report No. 184 (WMO/TD-No. 1473), Geneva, 29 pp.

Wong, C.S., J.R. Christian, S.-K. Emmy Wong, J. Page, Liusen Xie and S. Johannessen, 2010: Carbon dioxide in surface seawater of the eastern North Pacific Ocean (Line P), 1973–2005. *Deep-Sea Res. I*, 57(5):687–695, doi:10.1016/j.dsr.2010.02.003.

Contacts

[1] $W \cdot m^{-2}$ = watts per square metre.

[2] ppm = number of molecules of the gas per million molecules of dry air.

[3] ppb = number of molecules of the gas per billion (10^9) molecules of dry air.

[4] Indicated uncertainty ranges are calculated by a bootstrap method following Conway et al. (1994). This uncertainty is calculated with a confidence interval of 68% (one sigma).

[5] This percentage is calculated as the relative contribution of the mentioned gas(es) to the increase in global radiative forcing caused by all long-lived greenhouse gases since 1750.

[6] 1 PgC = 1 billion (10^9) tonnes or 10^{15} g of carbon.

[7] TgN = teragrams of nitrogen.

[8] ppt = number of molecules of the gas per trillion (10^{12}) molecules of dry air.

Selected greenhouse gas observatories

The Australian Tropical Atmospheric Research Station (ATARS) at **Gunn Point** (12.25°S, 131.05°E, 25 m a.s.l.) is located near Darwin, in Australia's Northern Territory. The station was established in 2010 and became a GAW regional station in 2012. It is co-located with a Bureau of Meteorology (BoM) research radar station and the operation is supported by both BoM and the Commonwealth Scientific and Industrial Research Organization (CSIRO, Australia). Gunn Point complements the growing atmospheric observation network in the Asian–Australian tropical region and is an important addition to the globally under-sampled tropical regions. Measurements currently include the main greenhouse and related trace gases (in situ CO_2, CH_4 and radon; a flask air sampling programme for CO_2, CH_4, N_2O, carbon monoxide (CO), hydrogen (H_2), $^{13}CO_2$, ^{18}OCO), as well as aerosol scattering coefficient, black carbon, ozone, NO_x, gaseous elemental mercury and short-lived halocarbons of tropical coastal marine origin. In the near future, measurement programmes will expand to include in situ N_2O, CO, particle number concentrations and volatile organic compounds.

Pha Din (21.57°N 103.52°E, 1466 m a.s.l.) is a recently designated GAW regional station. It is located on a hill in north-western Viet Nam above the surrounding forests. The facility is operated by the Vietnamese National Hydrometeorological Service. The site has been a meteorological station since 2011, when a tower was built to install a future meteorological radar. The laboratory building provides air-conditioned laboratory space and also basic accommodation for station operators and guest researchers. Capacities for continuous observations of greenhouse gases and aerosol optical properties were established in early 2014 through the collaboration of two Swiss institutes (Empa and the Paul Scherrer Institute), MeteoSwiss and the Vietnamese National Hydrometeorological Service. CO_2, CH_4 and CO are measured with cavity enhanced absorption spectroscopy. The Pha Din station is the first of its kind recording greenhouse gases, surface ozone and aerosol properties in a rural setting in Viet Nam.

JN 141841